

# Reactions between the $\text{SO}_4^{\cdot-}$ radical and some common anions in atmospheric aqueous droplets

OUYANG Bin, FANG Hao-jie, ZHU Cheng-zhu, DONG Wen-bo\*, HOU Hui-qi\*

(Laser Flash Photolysis Laboratory, Institute of Environmental Science, Fudan University, Shanghai 200433, China. E-mail: fdesi@fudan.edu.cn)

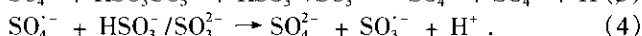
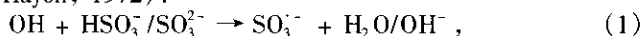
**Abstract:** The rate constants of reactions between the  $\text{SO}_4^{\cdot-}$  radical and some common anions in atmospheric aqueous droplets e. g.  $\text{Cl}^-$ ,  $\text{NO}_3^-$ ,  $\text{HSO}_3^-$  and  $\text{HCO}_3^-$  were determined using the laser flash photolysis technique. Absorption spectra of  $\text{SO}_4^{\cdot-}$  and the product radicals were also reported. The chloride ion was evaluated among all the anions to be the most efficient scavenger of  $\text{SO}_4^{\cdot-}$ . The results may supply useful information for a better understanding of the vigorous radical-initiated reactions in atmospheric aqueous droplets such as clouds, rains or fogs.

**Keywords:** sulfate radical; common anions; atmospheric aqueous-phase chemistry; radical chemistry

## Introduction

The conversion processes of some atmospheric pollutants inside the aqueous droplets e. g. clouds, rains and fogs present interesting topics to discuss. One typical example of this kind of pollutants was  $\text{SO}_2$ . It can dissolve into the droplets readily and then undergo aerobic oxidation process, during which it is finally converted to  $\text{SO}_4^{2-}$ . Much attention has been paid to this process because it is the main cause of acid rain.

It has been proposed that an important intermediate  $\text{SO}_4^{\cdot-}$  can be generated during the radical-initiated aerobic oxidation process of  $\text{SO}_2$ , as reactions (1)—(4) suggest (Hayon, 1972).



Once generated, the radical  $\text{SO}_4^{\cdot-}$  would react with the solutes in the aqueous droplets very rapidly due to its impressively high one-electron reduction potential  $E = 2.43$  V (Stanbury, 1989). Recently, George C. *et al.* selectively studied the reactions of  $\text{SO}_4^{\cdot-}$  with some organic substrates i. e. alcohols, ethers and esters in aqueous solution and suggested these to be possible sinks of  $\text{SO}_4^{\cdot-}$  in the atmospheric droplets (George, 2001). Considering the fact that the reduction potentials of many inorganic anion couples are lower than that of  $\text{SO}_4^{\cdot-} / \text{SO}_4^{2-}$ , reactions with these anions which are another abundant species in the atmospheric droplets are also expected to be important sinks of  $\text{SO}_4^{\cdot-}$ . But how fast do these reactions proceed? Among these anions which one would possess the highest possibility to scavenge  $\text{SO}_4^{\cdot-}$ ? These problems are still awaiting clarification.

The  $\text{SO}_4^{\cdot-}$  radical is of high reactivity. Reactions between this species and anions usually finish within the timescale from  $\mu\text{s}$  to  $\text{ms}$ , which makes the application of the laser flash photolysis technique to the research on this type of reactions appropriate and suitable. In this paper, we systematically studied the reactions between  $\text{SO}_4^{\cdot-}$  and some commonly occurring anions in the atmospheric droplets, hoping that it could provide useful kinetic information for the building of reaction models inside the clouds or rains etc. and in the meanwhile be helpful for a deeper understanding of the environmental behavior of  $\text{SO}_4^{\cdot-}$ .

## 1 Experimental

### 1.1 Laser flash photolysis apparatus

The excitation light was generated by the Quanta-Ray GCR-150 Nd:YAG laser operating at its 4th harmonic mode (266 nm, HRFM 5—6 ns, repetition rate 10 Hz, maximum

output energy 60 mJ/pulse, Q-switched, Spectra Physics). Other parts of the experimental setup have been described elsewhere (Ouyang, 2005).

### 1.2 Materials

$\text{K}_2\text{S}_2\text{O}_8$  ( $\geq 99.5\%$ , AR),  $\text{Na}_2\text{SO}_3$  ( $\geq 97\%$ , AR),  $\text{NaHCO}_3$  ( $\geq 99\%$ , AR),  $\text{KCl}$  ( $\geq 99.8\%$ , AR),  $\text{KBr}$  ( $\geq 99\%$ , AR),  $\text{KNO}_3$  ( $\geq 99\%$ , AR),  $\text{NaNO}_2$  ( $\geq 99\%$ , AR),  $\text{Na}_3\text{PO}_4$  ( $\geq 98\%$ , AR) were used as received. Wherever necessary,  $\text{KClO}_4$  (99.5%, AR) or  $\text{HClO}_4$  (70%—72%, AR) were added to adjust the ion strength or pH value of the target solution, respectively. Solutions were freshly prepared in triply distilled water. All experiments were carried out at  $(23 \pm 2)^\circ\text{C}$  under the flow conditions.

### 1.3 Derivation of $k_0$

Kinetic traces collected in the experiments were fitted according to the assumed mechanisms by the numerical integration method. As the least-square solutions were met, best-fit results and the corresponding rate coefficients were reported. All these steps were made by the Pro-Kineticist software (v 1.05, Applied Photophysics Ltd.).

According to the Debye-Hückel equation, the ion strength exerts influence upon the rate coefficient as:

$$\log k_i = \log k_0 - 1.02 Z_A Z_B I^{1/2} \quad (5)$$

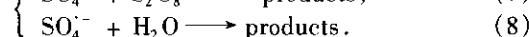
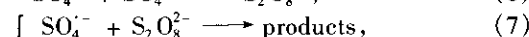
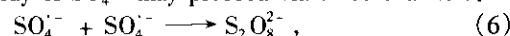
where  $I$  is the ion strength of the solution,  $Z_A$  and  $Z_B$  are the ionic charges,  $k_i$  is the rate coefficient at the specific  $I$  and  $k_0$  is the rate coefficient at infinite dilution. We could thereby transform the experimentally determined  $k_i$  to  $k_0$  using Equation (5) readily. It is noteworthy that Equation (5) is reasonable only when  $I < 0.15$ .

## 2 Results and discussion

### 2.1 Generation and the consequent decay of $\text{SO}_4^{\cdot-}$ after the laser flash photolysis of $\text{K}_2\text{S}_2\text{O}_8$

$\text{SO}_4^{\cdot-}$  was generated via the laser flash photolysis of aqueous solution of 0.01 mol/L  $\text{K}_2\text{S}_2\text{O}_8$  (about pH 6.0) by the 266 nm laser and its time-dependent decay curve at 440 nm (where one of its absorption peaks locates) is illustrated in Fig. 1.

The decay of  $\text{SO}_4^{\cdot-}$  may proceed via three channels:



Reaction (6) is in itself a second-order reaction while reactions (7) and (8) are pseudo-first order ones since both  $[\text{S}_2\text{O}_8^{2-}]$  and  $[\text{H}_2\text{O}]$  are much larger than  $[\text{SO}_4^{\cdot-}]$ . Fitting the decay curve in Fig. 1 using the pseudo-first order decay kinetics only failed to yield satisfactory result, suggesting that reaction (6) must have taken place significantly. A mixed pseudo-first and second order fitting method was therefore applied.

\* Corresponding author

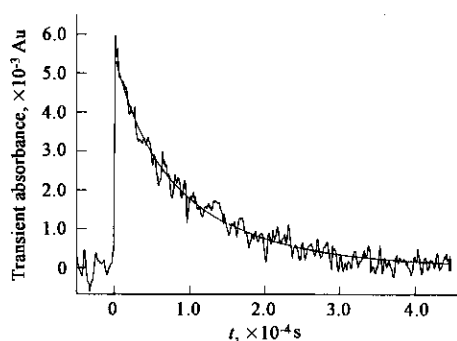


Fig.1 Absorption decay curve of  $\text{SO}_4^{\cdot -}$  at 440 nm with the mixed pseudo-first and second order best-fit

The initial concentration of  $\text{SO}_4^{\cdot -}$ , denoted as  $[\text{SO}_4^{\cdot -}]_0$ , was calculated from Equation (9)

$$[\text{SO}_4^{\cdot -}]_0 = \frac{A_{0,440\text{nm}}}{\epsilon_{\text{SO}_4^{\cdot -},440\text{nm}} \times l} \quad (9)$$

where  $A_{0,440\text{nm}}$  is the transient absorbance recorded at 400 nm at  $t = 0$ ,  $\epsilon_{\text{SO}_4^{\cdot -}}$  is the molar extinction coefficient of  $\text{SO}_4^{\cdot -}$  at 440 nm i. e.  $1600 \text{ (mol/L)}^{-1} \text{ cm}^{-1}$  (McElroy, 1990) and  $l$  is the optical path length 0.8 cm.

The best-fit result is shown in Fig.2, inside which the curve (a) is the pseudo-first order component with a corresponding rate  $k_7 \times [\text{S}_2\text{O}_8^{2-}] + k_8 = (7.3 \pm 0.3) \times 10^3 \text{ s}^{-1}$ , the curve (b) is the second order component with a rate coefficient  $k_6 = (8.8 \pm 1.1) \times 10^8 \text{ L/(mol} \cdot \text{s)}$  and curve (c) the overall decay curve. Taking the ion strength effect and  $k_8 = 5 \times 10^2 \text{ s}^{-1}$  (McElroy, 1990) into account, we obtained  $k_6$  and  $k_7$  at infinite dilution to be:  $k_{6(t=0)} = (5.8 \pm 0.7) \times 10^8$  and  $k_{7(t=0)} = (3.0 \pm 0.1) \times 10^5 \text{ L/(mol} \cdot \text{s)}$ .

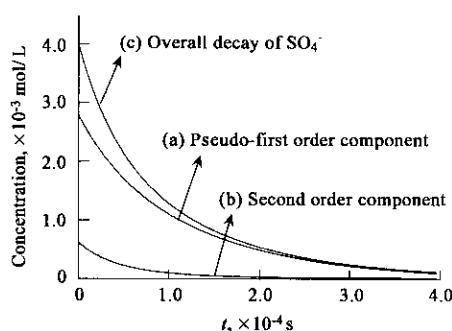
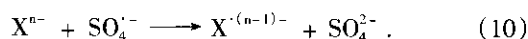


Fig.2 Separation of pseudo-first ( $\text{SO}_4^{\cdot -} + \text{S}_2\text{O}_8^{2-}$  and  $\text{SO}_4^{\cdot -} + \text{H}_2\text{O}$ ) and second order ( $\text{SO}_4^{\cdot -} + \text{SO}_4^{\cdot -}$ ) decay

## 2.2 Kinetics of reactions between $\text{SO}_4^{\cdot -}$ and different anions

Supposing an extra anion  $\text{X}^{n-}$  was introduced into the aqueous solution of  $\text{K}_2\text{S}_2\text{O}_8$  and was then subjected to the laser photolysis, a reaction will occur between  $\text{X}^{n-}$  and  $\text{SO}_4^{\cdot -}$  as:



Reaction (10) also follows the pseudo-first order mechanism since  $[\text{X}^{n-}]$  is still much larger than  $[\text{SO}_4^{\cdot -}]$ . Under this condition, reactions (6), (7), (8) and (10) are the four decay channels of  $\text{SO}_4^{\cdot -}$ . Since  $k_{6(t=0)}$ ,  $k_{7(t=0)}$  and  $k_8$  have been obtained in Section 2.1, curve fitting by Pro. K with these three values fixed will yield the pseudo-first order rate constant of reaction (10) at a specific  $[\text{X}^{n-}]$  easily. After correcting the ion strength effect, plotting these pseudo-first order rate constants against  $[\text{X}^{n-}]$  and fitting the plot

points with linear equation, the second-order rate constant of reaction (10) i. e.  $k_{10(t=0)}$  will be derived by reading the slope of the fit line.

In theory, we could either observe the decay curve of  $\text{SO}_4^{\cdot -}$  or the build-up curve of the product radical to determine the reaction rates. Under many circumstances, however, the absorption bands of  $\text{SO}_4^{\cdot -}$  and the product radical overlap. As a result, the monitoring wavelength was usually purposively set to be the one at which there was only one dominant absorber. This would remarkably simplify the kinetic analysis process.

The reaction rate constants derived in this work are summarized in Table 1.

Table 1 The summary of reaction rate constants

Reactions	$k$ ( $t = 0$ ), $\text{L/(mol} \cdot \text{s)}$
$\text{SO}_4^{\cdot -} + \text{Cl}^- \longrightarrow \text{SO}_4^{2-} + \text{Cl}^\cdot$	$(2.3 \pm 0.1) \times 10^8$
$\text{SO}_4^{\cdot -} + \text{NO}_3^- \longrightarrow \text{SO}_4^{2-} + \text{NO}_3^\cdot$	$(5.6 \pm 0.5) \times 10^4$
$\text{SO}_4^{\cdot -} + \text{OH}^- \longrightarrow \text{SO}_4^{2-} + \text{OH}^\cdot$	$(8.0 \pm 1.0) \times 10^7$
$\text{SO}_4^{\cdot -} + \text{HCO}_3^- \longrightarrow \text{SO}_4^{2-} + \text{CO}_3^{\cdot -} + \text{H}^\cdot$	$(1.8 \pm 0.2) \times 10^6$
$\text{SO}_4^{\cdot -} + \text{HSO}_3^- \longrightarrow \text{SO}_4^{2-} + \text{SO}_3^{\cdot -} + \text{H}^\cdot$	$(3.1 \pm 0.3) \times 10^8$
$\text{SO}_4^{\cdot -} + \text{SO}_3^{2-} \longrightarrow \text{SO}_4^{2-} + \text{SO}_3^{\cdot -}$	$(1.1 \pm 0.2) \times 10^8$
$\text{SO}_4^{\cdot -} + \text{NO}_2^- \longrightarrow \text{SO}_4^{2-} + \text{NO}_2^\cdot$	$(6.9 \pm 0.5) \times 10^8$
$\text{SO}_4^{\cdot -} + \text{Br}^- \longrightarrow \text{SO}_4^{2-} + \text{Br}^\cdot$	$(8.3 \pm 0.6) \times 10^8$
$\text{SO}_4^{\cdot -} + \text{HPO}_4^{2-} \longrightarrow \text{SO}_4^{2-} + \text{HPO}_4^{\cdot -}$	$(1.3 \pm 0.1) \times 10^6$ ( $I = 0.45$ )
$\text{SO}_4^{\cdot -} + \text{H}_2\text{PO}_4^- \longrightarrow$	No reaction observed

For measurement of the rate constant of the reaction between  $\text{SO}_4^{\cdot -}$  and  $\text{HPO}_4^{2-}$ , a high  $[\text{HPO}_4^{2-}]$  (0.1 mol/L) had to be applied for a clear observation of this reaction. The ion strength of this sample solution has obviously exceeded 0.15, so the transformation of  $k_t$  to  $k_0$  using Equation (5) was no longer reasonable. This explains why we only reported an uncorrected  $k$  of the reaction  $\text{SO}_4^{\cdot -} + \text{HPO}_4^{2-}$  in Table 1.

Table 1 shows the rate constants of reactions between anions and  $\text{SO}_4^{\cdot -}$  may vary as much as four orders of magnitude, indicating that the reactivity of these anions towards  $\text{SO}_4^{\cdot -}$  is different. It can be easily drawn from Table 1 that the magnitude of the rate constant does not simply rely on the reduction potential of the couple  $\text{X}^{(n-1)\cdot -}/\text{X}^{n-}$ . Taking  $\text{Cl}^-/\text{Cl}^\cdot$  and  $\text{SO}_3^{\cdot -}/\text{SO}_3^{2-}$  as an example; the reduction potential of the former couple (Schwarz, 1984) is much higher than that of the latter one (Merenyi, 1988), but  $\text{Cl}^-$  reduces  $\text{SO}_4^{\cdot -}$  faster than  $\text{SO}_3^{2-}$  does. The comparison between  $\text{Cl}^-/\text{Cl}^\cdot$  and  $\text{NO}_3^-/\text{NO}_3^\cdot$  is another interesting example: these two couples possess similar reduction potentials, i. e. 2.4 V (Schwarz, 1984) and (2.3—2.6) V (Neta, 1986) respectively, but the reaction rate constant of  $\text{Cl}^- + \text{SO}_4^{\cdot -}$  is by four orders of magnitude higher than that of  $\text{NO}_3^- + \text{SO}_4^{\cdot -}$ . The causes of such inversions may be many. Among them some accepted arguments were: (1) Reactions such as  $\text{SO}_4^{\cdot -} + \text{NO}_3^-$  may belong to the inner-sphere electron transfer type, which renders the electron transfer process be rather difficult (Huie, 1984); (2) Necessary stretching or bending of the reactants may bring extra energy-barrier to the reactions like  $\text{SO}_4^{\cdot -} + \text{NO}_2^-$  (Stanbury, 1984). Moreover, reactions like  $\text{SO}_4^{\cdot -} + \text{NO}_2^-$  (or  $\text{SO}_3^{\cdot -}$  and  $\text{HSO}_3^-$ ) may have fallen into the Marcus-Inverted regions due to the relatively high  $\Delta E$  ( $\Delta E$  is the reduction potential difference between the couples  $\text{SO}_4^{\cdot -}/\text{SO}_4^{2-}$  and  $\text{X}^{(n-1)\cdot -}/\text{X}^{n-}$ ), which will also lead to an opposite changing direction of  $k$  and  $\Delta E$ .

## 2.3 UV-Vis absorption spectra of $\text{SO}_4^{\cdot -}$ and the product radicals

The molar extinction coefficients of the product radical  $\text{X}^{(n-1)\cdot -}$  at the wavelength  $\lambda$ , denoted as  $\epsilon_{\text{X}^{(n-1)\cdot -}, \lambda}$  can be

calculated via the following equation:

$$\epsilon_{X^{(n-1)^{\cdot-}}, \lambda} = \frac{A_{X^{(n-1)^{\cdot-}}, \lambda} \times \epsilon_{SO_4^{\cdot-}, \lambda}}{A_{SO_4^{\cdot-}, \lambda} \times (SO_4^{\cdot-})\%}, \quad (11)$$

where  $A_{X^{(n-1)^{\cdot-}}, \lambda}$  is the transient absorbance of the product radical  $X^{(n-1)^{\cdot-}}$  recorded at the wavelength  $\lambda$  immediately after the decay of  $SO_4^{\cdot-}$  was over,  $\epsilon_{SO_4^{\cdot-}, \lambda}$  is the molar

extinction coefficient of  $SO_4^{\cdot-}$  at  $\lambda$ ,  $A_{SO_4^{\cdot-}, \lambda}$  is the starting transient absorbance of  $SO_4^{\cdot-}$  at  $\lambda$  and  $(SO_4^{\cdot-})\%$  is the percentage of  $SO_4^{\cdot-}$  consumed via Reaction (10) in the entire  $SO_4^{\cdot-}$ . The calculation of  $(SO_4^{\cdot-})\%$  was performed by the Pro.K software.

The spectra are shown in Fig. 3.

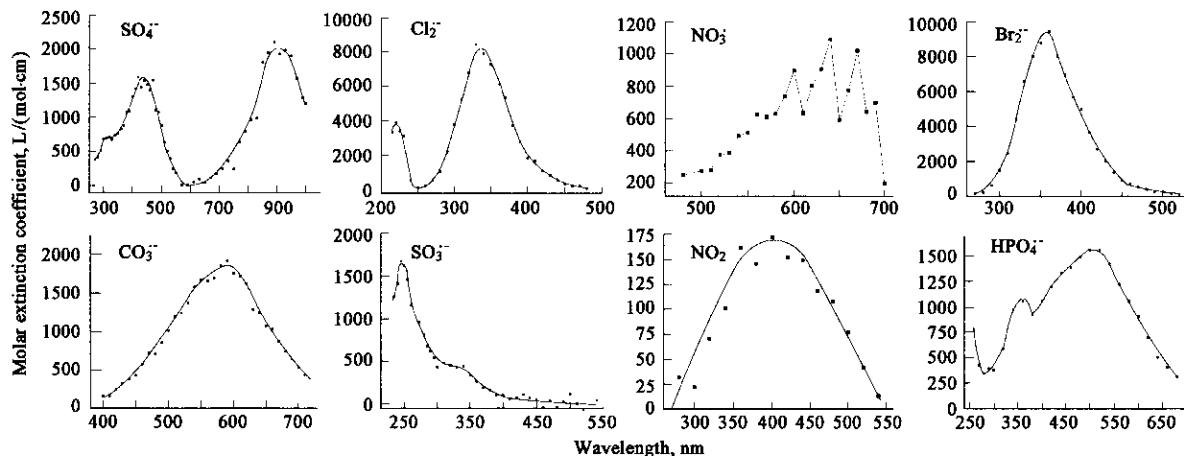


Fig. 3 UV-Vis absorption spectra of the radicals

Admittedly, we were unable to record the absorption spectra of  $Cl^{\cdot}$  and  $Br^{\cdot}$  in this work because these two radicals combined quickly with  $Cl^-$  and  $Br^-$  in aqueous solution and then formed  $Cl_2^{\cdot-}$  and  $Br_2^{\cdot-}$ . Therefore, only the absorption spectra of  $Cl_2^{\cdot-}$  and  $Br_2^{\cdot-}$  were reported here. Observation of these two radicals was relatively easy due to their extraordinarily high  $\epsilon_{max}$  (about  $1 \times 10^4$  L/(mol·cm)). The  $\epsilon_{max}$  of some other radicals e.g.  $NO_3^{\cdot}$ ,  $CO_3^{\cdot-}$  and  $SO_3^{\cdot-}$  were in similar ranges, from  $1 \times 10^3$  L/(mol·cm) to  $2 \times 10^3$  L/(mol·cm). The  $\epsilon_{max}$  of  $NO_2^{\cdot}$  was the lowest among all of the radicals ( $< 200$  L/(mol·cm)).

As shown in Fig. 3, the inorganic radicals exhibit quite different absorption characteristics, which render the identification of them in the laser flash photolysis experiments very easy. Hopefully the information contained in Fig. 3 will facilitate future investigations on the chemical behavior of these radicals in environment.

## 2.4 Atmospheric implications

The reaction possibility of a specific anion with  $SO_4^{\cdot-}$  depends on two factors, one being the reaction rate constant and the other the concentration of this anion in droplets.

$NO_3^-$  is one of most popular anions in the clouds or rain droplets. The reaction possibility of this anion with  $SO_4^{\cdot-}$  is, nevertheless, of minor importance due to the relatively low reaction rate constant of  $NO_3^- + SO_4^{\cdot-}$ . Other anions e.g.  $HSO_3^-$ ,  $Br^-$  and  $NO_2^-$  react with  $SO_4^{\cdot-}$  much faster than  $NO_3^-$  does, but their reaction possibility with  $SO_4^{\cdot-}$  is again limited by their low concentrations in droplets. Therefore none of the above anions can be considered as an equally important sink of  $SO_4^{\cdot-}$  as  $Cl^-$ , which has both a moderately high concentration (about  $10^{-4}$  mol/L in clouds and maybe even higher in the marine environment) and a high reaction rate constant ( $2.3 \times 10^8$  L/(mol·s)) with  $SO_4^{\cdot-}$ .

As already noted in Section 2.2, oxidation of  $Cl^-$  by

$SO_4^{\cdot-}$  would produce  $Cl_2^{\cdot-}$  in the aqueous droplets. The reduction potential of the couple  $Cl_2^{\cdot-}$  is higher than that of the  $SO_3^{\cdot-}/SO_3^{2-}$  one, which implies that the auto-oxidation chain reaction of  $SO_2$  (as Equations (1)–(4) indicate) will still be propagated even though  $Cl^-$  has intercepted most of the  $SO_4^{\cdot-}$ .

## References:

- George C, El Rassy H, Chovelon J M, 2001. Reactivity of selected volatile organic compounds (VOCs) toward the sulfate radical ( $SO_4^{\cdot-}$ ) [J]. *Int J Chem Kinet*, 33(9): 539–547.
- Hayon E, McGarvey J J, 1967. Flash photolysis in the vacuum ultraviolet region of sulfate, carbonate, and hydroxyl ions in aqueous solutions [J]. *J Phys Chem*, 71(5): 1472–1477.
- Hayon E, Treinin A, Wilf J, 1972. Electronic spectra, photochemistry, and autoxidation mechanism of the sulfite-bisulfite-pyrosulfite systems.  $SO_2^{\cdot-}$ ,  $SO_3^{\cdot-}$ ,  $SO_4^{\cdot-}$ , and  $SO_5^{\cdot-}$  radicals [J]. *J Am Chem Soc*, 94(1): 47–57.
- Huie R E, Neta P, 1984. Chemical behavior of  $SO_3^{\cdot-}$  and  $SO_5^{\cdot-}$  radicals in aqueous solutions [J]. *J Phys Chem*, 88(23): 5665–5669.
- McElroy W J, 1990. A laser photolysis study of the reaction of  $SO_4^{\cdot-}$  with  $Cl^-$  and the subsequent decay of  $Cl_2^{\cdot-}$  in aqueous solution [J]. *J Phys Chem*, 94(6): 2435–2441.
- McElroy W J, Waygood S J, 1990. Kinetics of the reactions of the  $SO_4^{\cdot-}$  radical with  $SO_4^{\cdot-}$ ,  $S_2O_8^{2-}$  and  $Fe^{2+}$  [J]. *J Chem Soc Faraday Trans*, 86(14): 2557–2564.
- Merenyi G, Lind J, Shen X, 1988. Electron transfer from indoles, phenol, and sulfite ( $SO_3^{2-}$ ) to chlorine dioxide ( $ClO_2$ ) [J]. *J Phys Chem*, 92(1): 134–137.
- Neta P, Huie R E, 1986. Rate constants for reactions of nitrogen oxide radicals in aqueous solutions [J]. *J Phys Chem*, 90(19): 4644–4648.
- Ouyang B, Dong W B, Hou H Q, 2005. A laser flash photolysis study of nitrous acid in the aqueous phase [J]. *Chem Phys Lett*, 402: 306–311.
- Schwarz H A, Dodson R W, 1984. Equilibrium between hydroxyl radicals and thallium (II) and the oxidation potential of hydroxyl(aq) [J]. *J Phys Chem*, 88(16): 3643–3647.
- Stanbury D M, Lednický L A, 1984. Outer-sphere electron-transfer reactions involving the chlorite/chlorine dioxide couple. activation barriers for bent triatomic species [J]. *J Am Chem Soc*, 106(10): 2847–2853.
- Stanbury D M, 1989. Reduction potentials involving inorganic free radicals in aqueous solution [J]. *Adv Inorg Chem*, 33: 69–138.

(Received for review December 12, 2004. Accepted March 10, 2005)